Steel and Composite Structures, *Vol. 20, No. 1 (2016) 43-56*
DOI: http://dx.doi.org/10.12989/scs.2016.20.1.043

Experimental study of anisotropic behavior of PU foam used in sandwich panels

Monika Chuda-Kowalska [*1] and Andrzej Garstecki [2a]

[1] *Institute of Structural Engineering, Poznan University of Technology pl. Sklodowskiej-Curie 5, 60-965 Poznan, Poland*
[2] *Stanislaw Staszic University of Applied Sciences in Pila, ul. Podchorazych 10, 64-920 Pila, Poland*

(*Received January 24, 2015, Revised July 01, 2015, Accepted July 08, 2015*)

Abstract. Polyurethane foam with low density used in sandwich panels is examined in the paper. A series of experiments was carried out to identify mechanical parameters of the foam. Various experimental methods were used for determining the shear modulus, namely a four and three point bending tests (the most common in engineering practice), a double-lap shear test and a torsion test. The behavior of PU in axial compression and tension was also studied. The experiments revealed pronounced anisotropy of the PU foam. An orthotropic model is proposed. Limitations of application of isotropic model of PU in engineering practice is also discussed.

Keywords: polyurethane foam; anisotropy; sandwich panels; material model; experimental methods

1. Introduction

Sandwich panels with the core made of a porous material are widely and still increasingly applied in civil engineering because of their extraordinary attractive features: good thermal insulation, very small self-weight, good bearing capacity and small cost of production, transport and erection. There is strong tendency to apply these panels of larger span lengths and to use them as bracing of purlins or frames. Therefore, a number of papers have been devoted to design (Hassinen *et al*. 1997, Pokharel and Mahendran 2005, Gosowski and Gosowski 2014) and optimization of sandwich beams and plates (Awad 2013, Studzinski *et al*. 2013). It has also been a good motivation for further research with the aim to develop the methods of testing the whole panel (Xie *et al*. 2014, Studzinski *et al*. 2015) or focus on mechanical parameters of the soft core (Jin *et al*. 2007, Caliri Júnior *et al*. 2012, Chuda-Kowalska *et al*. 2015) and their numerical simulation (Tita and Caliri Júnior 2012). These parameters usually are determined in a macro scale approach (Liu and Subhash 2004, Chen and Fatt 2013) but micro mechanical methods have also been used (Gibson and Ashby 1997, Janus-Michalska and Pecherski 2003, Subramanian and Sankar 2012).

In this paper the PU foam with a closed-cell structure and approximately 40 kg/m^3 density used in sandwich panels is analyzed. Common application of these panels in civil engineering implies

*Corresponding author, Assistant Professor, E-mail: monika.chuda-kowalska@put.poznan.pl
[a] Professor, E-mail: andrzej.garstecki@put.poznan.pl

 ISSN: 1229-9367 (Print), 1598-6233 (Online)

specific design and testing procedures accounting for the influence of the week core on the behavior of the layered structure (Zenkert 1995, Davies 2001). The assumption of isotropy and linear elasticity is very convenient from engineering point of view and it is frequently used and developed (Gibson 2011). Then the shear modulus of the core material G_C plays a crucial role for structural performance of a sandwich panel (Chuda-Kowalska *et al*. 2010, Juntikka and Hallstorm 2007). Therefore, establishing of reliable experimental methods for determining the shear modulus of the core is important. Three layered sandwich plate can play the role of an element restraining a thin walled beam from torsional instability. A semi rigid contact can be modeled by the way of elastic springs similarly as it is done in case of corrugated steel plates (Rzeszut *et al*. 2014).

The authors carried out a series of experiments with the aim to identify the shear modulus of the PU foam used in sandwich panels. Typically, G_C is determined in a bending test of the panel. The dimensions of the plate and the loading in this test allow to analyze the results in frame of the Ordinary Sandwich Panel Theory thoroughly described by Allen (1969) and Plantema (1966) and briefly summarized by Zenkert (1995). Since the thickness and elasticity moduli of the thin steel facings can be determined in classical tension test, the measured deflection of the plate provides sufficient information for evaluation of G_C. The authors identified this parameter also in a torsion test and in a double-lap shear test. The latter one had two options with and without constraint of the lateral displacements.

The manufacturing process of sandwich panels produced for civil engineering can have vast influence on the microstructure and behavior of the core material because steel facings limit the growth of foam in the thickness direction. In the authors' opinion this is the reason of the anisotropy of the core material observed in the experiments reported in the paper.

In Chapter 2 the results of various types of tests are presented and discussed. The tests and the interpretation of the results were based on the assumption of isotropy and referred to recommendations of the Eurocode EN 14509. The differences in results obtained from various types of tests are shown and discussed in detail. Moreover, it was demonstrated that the assumption of the isotropy of PU foam appeared to be inconsistent. Chapter 3 presents another series of tests done with the aim to study the homogeneity of material parameters across the width of panels and orthotropy of the foam. An orthotropic model was proposed in Chapter 4. Numerical examples were presented in Chapter 5.

2. Experimental approach for isotropic model

For the examined sandwich panels with PU foam core the standard experimental methods used to estimate material parameters of the core (E_C, G_C) are described in EN 14509. They are based on the assumption that the materials of steel facings and the core are isotropic, homogeneous and linearly elastic. The Young's modulus E_S of the steel is evaluated in typical tension tests. The shear modulus G_C of the core is identified in various tests. The authors used tests illustrated in Fig. 1 and described in detail by Chuda-Kowalska (2013).

The method of determination of the shear modulus G_C from a bending test is based on the Ordinary Sandwich Plate Theory. The total displacement f of the mid-point of the span of the panel can be decomposed into a flexural component w_B due to the bending moment, a shear component w_S due to the shear force and w_0 which results from the compression of the panel at the support

$$f = w_B + w_S + w_0 = w + w_0, \tag{1}$$

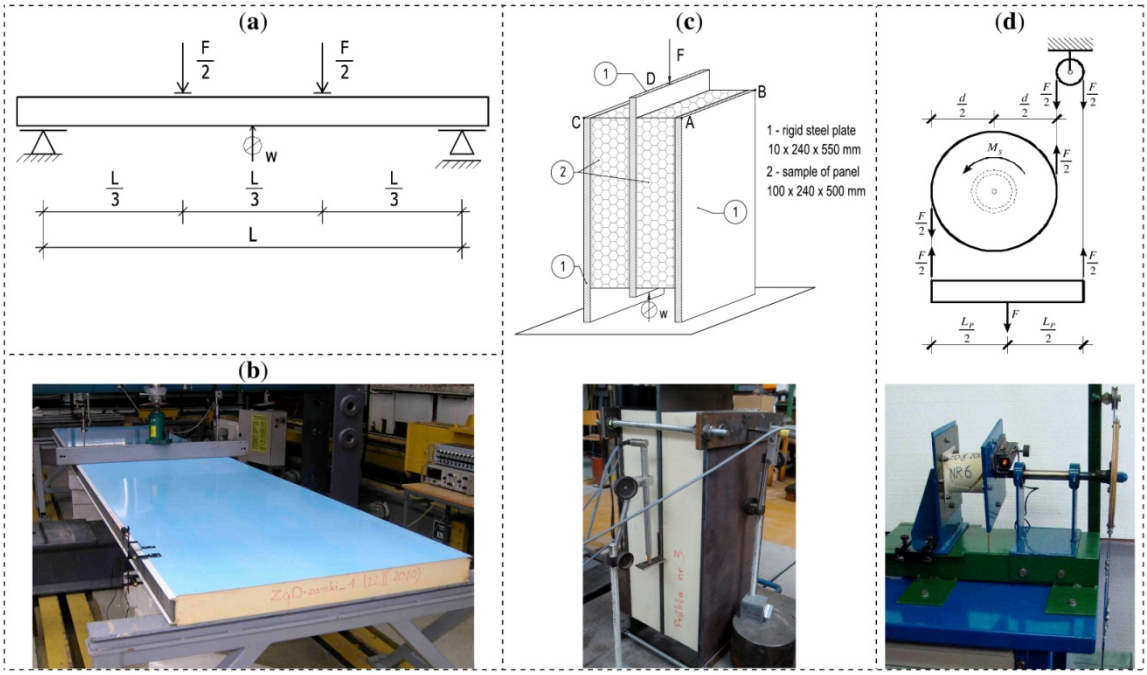

Fig. 1 Set up for various shear tests: (a) four-point bending test; (b) three-point bending test; (c) double-lap shear test with and without constraint at the edges A-B and C-D; (d) torsion test

The method of determination of the shear modulus G_C from a bending test is based on the Ordinary Sandwich Plate Theory. The total displacement f of the mid-point of the span of the panel can be decomposed into a flexural component w_B due to the bending moment, a shear component w_S due to the shear force and w_0 which results from the compression of the panel at the support

$$w_B = \frac{23 \cdot F \cdot L^3}{1296 \cdot EI}, \qquad w_S = \frac{F \cdot L}{6 \cdot G_C \cdot A_C} \qquad \Rightarrow \qquad G_C = \frac{F \cdot L}{6 \cdot B \cdot d_C \cdot w_S}, \tag{2}$$

The method of determination of the shear modulus G_C from a bending test is based on the Ordinary Sandwich Plate Theory. The total displacement f of the mid-point of the span of the panel can be decomposed into a flexural component w_B due to the bending moment, a shear component w_S due to the shear force and w_0 which results from the compression of the panel at the support.

$$w_B = \frac{F \cdot L^3}{48 \cdot EI}, \qquad w_S = \frac{F \cdot L}{4 \cdot G_C \cdot A_C} \qquad \Rightarrow \qquad G_C = \frac{F \cdot L}{4 \cdot B \cdot d_C \cdot w_S}. \tag{3}$$

In double-lap shear tests (test **c** in Fig. 1) the shear modulus is determined basing on the assumption that pure shear stress fields exist in the PU core. It leads to Eq. (4)

$$G_C = \frac{F \cdot d_C}{2 \cdot w \cdot B \cdot L}, \tag{4}$$

where B, L and d_C denote the width, length and depth of the core of one specimen, respectively. In our tests there were dimensions: B = 240 mm, L = 500 mm and d_C = 100 mm. The pure shear assumption is not perfectly satisfied because there exists an eccentricity of active load and reaction forces which produce a bending effect. To evaluate this effect the authors tested three samples with lateral constraints at the upper and lower edges and three with unconstrained upper edge. This disturbance for materials subjected to large deformation was analyzed e.g., by Ziolkowski (2006). Note that the double-lap test is not commonly used for sandwich panels because of time consuming sample preparation.

The experimental set-up for the torsion test is illustrated in Fig. 1 (test **d**). The cylindrical specimen had two steel head plates. One was rigidly fixed and the second rotatable. The angle of rotation φ was measured using laser pointer attached to the rotating head plate and pointing at the precise leveling staff. The sample was loaded by the torque M_S. The shear modulus G_C was calculated from Eq. (5)

$$\varphi = \frac{M_S \cdot L}{G_C \cdot I_0}, \tag{5}$$

where B, L and d_C denote the width, length and depth of the core of one specimen, respectively. In our tests there were dimensions: B = 240 mm, L = 500 mm and d_C = 100 mm. The pure shear assumption is not perfectly satisfied because there exists an eccentricity of active load and reaction forces which produce a bending effect. To evaluate this effect the authors tested three samples with lateral constraints at the upper and lower edges and three with unconstrained upper edge. This disturbance for materials subjected to large deformation was analyzed e.g., by Ziolkowski (2006). Note that the double-lap test is not commonly used for sandwich panels because of time consuming sample preparation.

The experimental set-up for the torsion test is illustrated in Fig. 1 (test **d**). The cylindrical specimen had two steel head plates. One was rigidly fixed and the second rotatable. The angle of rotation φ was measured using laser pointer attached to the rotating head plate and pointing at the precise leveling staff. The sample was loaded by the torque M_S. The shear modulus G_C was calculated from Eq. (5).

All three bending tests summarized in Table 1 (a.1, a.2, b) were carried out strictly following the recommendations of EN 14509. Four-point bending tests (**a.1**) were carried out on beam-like

Table 1 The shear modulus G_C of the PU foam

	Type of test (Fig. 1)					
	Bending			**Double-lap**		**Torsion**
	(a.1)	**(a.2)**	**(b)**	**(c.1)**	**(c.2)**	**(d)**
	3.41	4.73	4.61	2.98	2.95	2.61
	3.48	4.80	4.83	3.04	2.93	2.59
$\boldsymbol{G_C}$ [MPa]	3.15	4.64	4.74	3.02	2.91	2.75
	3.32	-	-	-	-	2.63
	3.29	-	-	-	-	2.76
Mean value	**3.33**	**4.72**	**4.73**	**3.01**	**2.93**	**2.67**
Standard deviation	0.11	0.07	0.09	0.02	0.02	0.07

Table 2 The influence of longitudinal edge profiling

	(**a.2**)	(**b**)
G_C **[MPa] –** samples with edge profiling	4.72	4.73
G_C **[MPa] –** samples without edge profiling	3.81	3.85

strips with L_0 = 0.9 m and B = 0.1 m. The compression w_0 in Eq. (1) is neglected according to EN 14509. Four-point bending tests (**a.2**) were carried out on short panels with edge profiling, L_0 = 0.9 m and B = 1.1 m (w_0 was taken into account). Three-point bending tests (**b**) were carried out on long panels with edge profiling, L_0 = 4.9 m, B = 1.1 m (w_0 in Eq. (1) was neglected).

Comparing the results of the test (**a.2**) with (**b**) we observe that in 3-point bending test on long panels (test **b**) the term w_0, representing compression of the core at the support, is truly negligible. However, let us underline that the longitudinal edge profiling existing in samples of actual width of the panel results in increased stiffness of samples, that violates assumption of idealized sandwich beam used in derivation of formulas (2) and (3). In effect the shear modulus G_C computed from Eqs. (2) or (3) is overestimated (Chuda-Kowalska 2012) because it includes the influence of the edge profiling. It can be referred to as equivalent modulus G_C. Practical design engineers introduce this equivalent G_C into OSAPT theory without accurate consideration of edge profiling. It is acceptable in analyses of global response of panels. Nevertheless, results of tests (**a.2**) and (**b**) do not represent the true shear modulus G_C of PU foam. In the analyses of local effects e.g., local instability of the facing, the true modulus G_C should be introduced to FEM analyses.

In order to examine the influence of the edge profiling on the estimated value of G_C, the samples with cut out edge profiling were tested, too. The results are presented in Table 2.

Table 2 demonstrates that G_C is overestimated by approx. 20% when the samples have the edge profiling. The true shear modulus of PU foam was G_C = 3.81 MPa and 3.85 MPa. A similar value was evaluated when in Table 1, test (**a.1**) the compression of the core at supports was taken into account. Concluding this discussion test (**a.1**) deserves recommendation with obligatory measurement of w_0 representing the compression of the core at the supports.

Next, we focus our attention on the Young's modulus E_C of the core material. It will be determined in tension/compression tests on cubic samples containing the core material and facings according to the appropriate procedure recommended in EN 14509. The samples had dimensions 100×100×100 mm. The results of tests are presented in Table 3.

Note that the PU material in the core of the panel has 6% lower Young's modulus E_C in tension than in compression. One can expect that it has no influence on the properties of sandwich panels in bending, but it is an open question how it influences the local stability of the compressed facing. Anyway, if the same value of E_C is to be assigned to tension and compression the authors recommend to assume the arithmetic mean of two types of tests.

During compression and tension tests we made next observation, namely that the Poisson's

Table 3 Young's modulus E_C determined in tension and compression tests

	E_C [MPa]	Standard deviation [MPa]
Tension	3.59	0.17
Compression	3.82	0.44

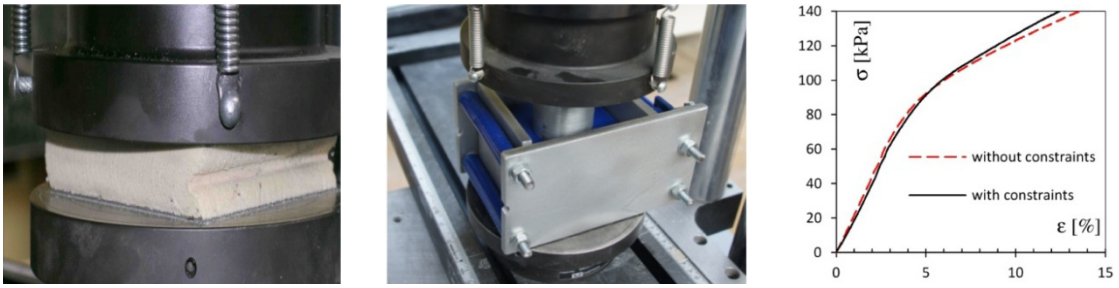

(a) (b) (c)

Fig. 2 Compression test: (a) without lateral constraints; (b) with constraints; (c) σ-ε relationship

ratio ν_C is near to zero even for strains exceeding the elastic range. The value of $\nu_C \cong 0$ was confirmed when we carried out next series of compression tests without (Fig. 2(a)) and with (Fig. 2(b)) constraint on lateral strains. It appeared that this constraint slightly affected the σ - ε relationship only in the range of large strains (Fig. 2(c)).

Concluding this chapter let us underline that the linear elastic and isotropic model of PU foam is very attractive for engineers and therefore, it is commonly used. It has only two constants E_C and G_C or E_C and Poisson's ratio ν_C, because the relation Eq. (6) must obligatory hold in this classical model.

$$G = \frac{E}{2(1+\nu)} \tag{6}$$

However, it appears that when we introduce E_C and G_C identified in the tests described above, then Eq. (6) is not satisfied, because it provides negative values of the ratio ν_C. Alternatively, when we introduce $\nu_C = 0$ and the identified E_C , then G_C obtained from Eq. (6) does not match results of tests. This proves that the linear elastic and isotropic model of PU foam is inconsistent. One must be aware of this fact when using this model.

3. Homogeneity and anisotropy of the PU foam

To study the homogeneity and anisotropy of the PU foam, a new series of samples was prepared by the same manufacturer.

The first group of tests was planned with the aim to check whether the material parameters depend on the location of the sample in the width direction of the panel. Cubic samples 100×100×100mm were cut out at points 1, 1a at the boundary and 3, 4 near the midpoint of the width (Fig. 3). All samples were cut out at points with a similar coordinate X. The samples had removed both steel facing layers and were subjected to tension in Z direction. The Young's modulus obtained in 24 tests is presented in Table 4. Remarkable discrepancy of the results is observed. Differences in E_{Ct} appear between both boundary groups $Z1$ and $Z1a$ and between both interior groups $Z3$ and $Z4$. Differences in E_{Ct} within each group (columns in Table 4) also appear. We conclude that there is a random scatter of Young's modulus of the foam reaching 6%. This fact should be taken into account in the analysis of local effects e.g., bubbles. In other analyses the mean values of material parameters can be used.

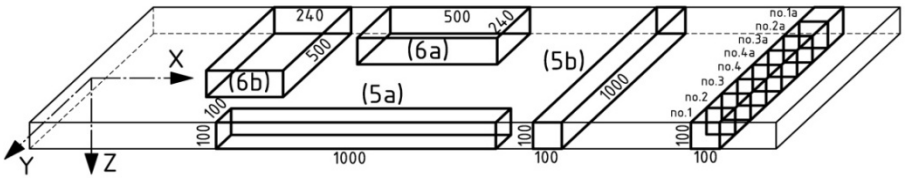

Fig. 3 Position of samples cut out from the panel and notation of principal directions *X*,*Y*,*Z*

Table 4 Characteristic values obtained from tension test in Z direction for different sample's positions

	No.Z1			***No.Z1a***			***No.Z3***			***No.Z4***		
	E_{C_t} [MPa]	$f_{C_t}^{\max}$ [kPa]	$\varepsilon_{C_t}^{\max}$ [%]	E_{C_t} [MPa]	$f_{C_t}^{\max}$ [kPa]	$\varepsilon_{C_t}^{\max}$ [%]	E_{C_t} [MPa]	$f_{C_t}^{\max}$ [kPa]	$\varepsilon_{C_t}^{\max}$ [%]	E_{C_t} [MPa]	$f_{C_t}^{\max}$ [kPa]	$\varepsilon_{C_t}^{\max}$ [%]
	3.39	82.12	2.40	3.56	99.13	2.82	3.37	106.42	3.28	3.54	107.12	3.01
	3.40	71.01	2.00	3.48	87.95	2.53	3.48	97.30	2.87	3.55	134.52	3.68
	3.31	98.37	3.10	3.60	96.69	2.78	3.42	91.04	2.66	3.60	88.23	2.44
	3.34	84.88	2.54	3.42	99.76	3.05	3.28	97.79	2.99	3.47	96.57	2.85
	3.36	86.65	2.61	3.36	95.42	2.96	3.32	111.96	3.47	3.49	104.64	3.13
	3.27	92.25	2.90	3.37	90.19	2.71	3.34	94.38	2.88	3.48	128.37	3.78
$\bar{k}$	**3.35**	**85.88**	**2.59**	**3.47**	**94.86**	**2.81**	**3.37**	**99.81**	**3.02**	**3.52**	**109.91**	**3.15**
δ	0.05	9.31	0.38	0.10	4.81	0.18	0.07	7.85	0.30	0.05	18.06	0.51

Table 5 Results of axial tests in directions *X*, *Y* and *Z*

		X			***Y***			***Z***		
		n	$\bar{k}$	δ	*n*	$\bar{k}$	δ	*n*	$\bar{k}$	δ
TENSION	E_{C_t} [MPa]	6	14.33	0.33	6	6.80	0.13	24 (Table 4)	3.43	0.07
	$f_{C_t}^{\max}$ [kPa]		180.40	52.09		161.40	23.68		97.62	10.01
	$\varepsilon_{C_t}^{\max}$ [%]		1.32	0.41		2.29	0.31		2.89	0.34
COMPRESSION	E_{C_c} [MPa]	3	13.45	0.20	3	4.41	0.21	3	3.65	0.09
	$f_{Cc}^{0.02}$ [kPa]		223.93	3.91		83.69	4.29		66.48	1.53
	$f_{Cc}^{0.1}$ [kPa]		240.38	2.26		151.79	5.58		129.82	2.33

In Table 4 the notation was used: E_{Ct}, $f_{Ct}^{\max}$ - Young's modulus and tensile strength, respectively, $\varepsilon_{Ct}^{\max}$ - strain corresponding to the tensile strength, $\bar{k}$ - mean value and δ - standard deviation.

The second group of tests was performed in order to assess experimentally the anisotropy. Nine types of tests were carried out, namely axial tension (E_{Ct}, $f_{Ct}^{\max}$, $\varepsilon_{Ct}^{\max}$) and compression (E_{Cc}, $f_{Cc}^{0.02}$, $f_{Cc}^{0.1}$ - Young's modulus and compressive strength of the core material for the strain levels ε = 2% and 10%, respectively – EN 14509) in three orthogonal directions. The numbers of tested samples *n* and the values received from these tests are shown in Table 5.

The behavior of the tested samples significantly depended on the stress direction. In tension test rapid failure of specimens was observed. Therefore, it was possible to evaluate the parameters $f_{Ct}^{\max}$ and $\varepsilon_{Ct}^{\max}$. This kind of failure is usually initiated at the weakest point of the microstructure of the foam and therefore, large differences in ultimate load for various samples appeared. Contrariwise, in compression test the specimens did not exhibit a well-defined ultimate load and thus material parameters shown in Table 5 were calculated for the specific strain values. Therefore, the standard deviation factors for compression are smaller compared to tension. Stress-strain relations for compression are shown in Fig. 4. Note that in the elasticity region (Fig. 4(b)) similar E_{Cc} is observed for Y and Z directions, but linear ranges are different. The yield strength in X, direction is higher (Fig. 4(a)). Averaged results of tension tests are shown in Fig. 5.

Further types of tests were planed aiming at determination the shear moduli G_{ZX} and G_{YZ}. We carried out four-point bending tests and double-lap shear tests. The samples (Figs. 5(a), 5(b), 6(a) and 6(b)) were cut out from the sandwich slab in respective orientations shown in Fig. 3. As

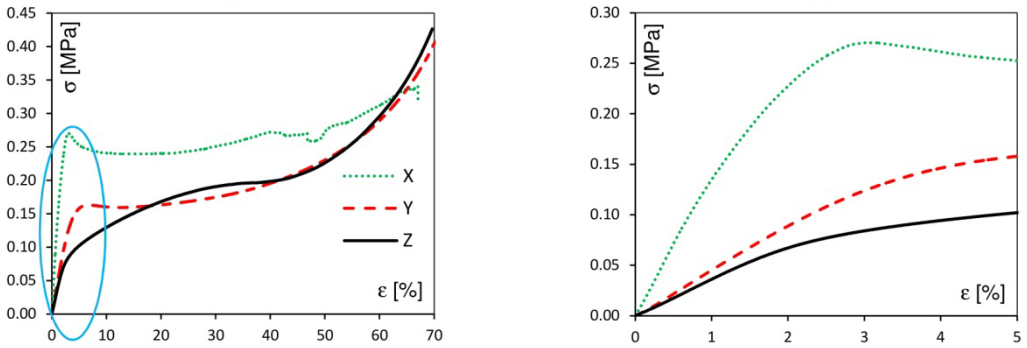

Fig. 4 Compression test, σ-ε plots for X, Y and Z directions: (a) full range of strain; (b) close-up of initial state

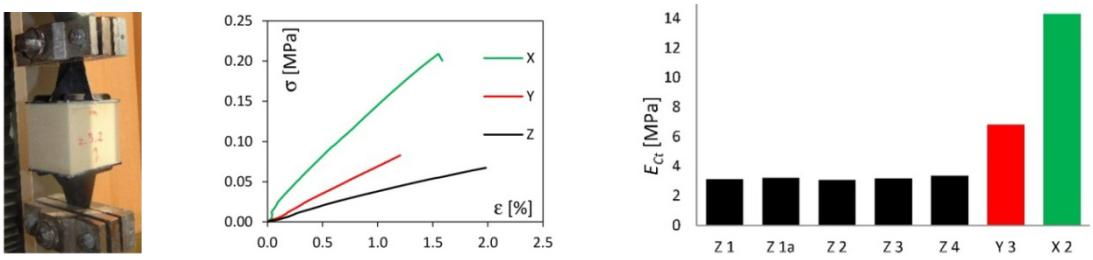

Fig. 5 Tension tests: (a) experimental set-up; (b) σ-ε relationship; (c) E_{Ct} in X, Y and Z directions. Numbers of tests 1, 1a, 2, 3, 4 refer to Fig. 3 and indicate the position of the sample

Table 6 Experimental results of G

	G_{ZX} [MPa]	G_{YZ} [MPa]	δ [%]
Double-lap shear test	2.49	2.20	13.18
Four-point bending test	**3.00**	**2.30**	30.43

previously, the double-lap shear test gave lower shear moduli G than the bending test. However, both types of tests revealed a pronounced anisotropy of the material.

4. Experimental approach for orthotropic model

The experiments described in Chapter 3 showed that PU foam manifests evident anisotropy. In this Chapter an orthotropic model will be proposed. The principal axes of orthotropy will coincide with the directions X, Y and Z shown in Fig. 3.

We limit considerations to linear-elasticity. We also assume symmetry of stress and strain tensors and positive definiteness of the strain energy. In this case the generalized Hooke's law can be written in contracted engineering notation of stresses and strains as

$$\varepsilon_i = S_{ij}\sigma_j, \qquad i,j = 1,2,3 \tag{7}$$

The experiments described in Chapter 3 showed that PU foam manifests evident anisotropy. In this Chapter an orthotropic model will be proposed. The principal axes of orthotropy will coincide with the directions X, Y and Z shown in Fig. 3.

We limit considerations to linear-elasticity. We also assume symmetry of stress and strain tensors and positive definiteness of the strain energy. In this case the generalized Hooke's law can be written in contracted engineering notation of stresses and strains as

$$\begin{bmatrix} \varepsilon_X \\ \varepsilon_Y \\ \varepsilon_Z \\ \gamma_{XY} \\ \gamma_{YZ} \\ \gamma_{ZX} \end{bmatrix} = \begin{bmatrix} 1/E_X & -\nu_{YX}/E_Y & -\nu_{ZX}/E_Z & 0 & 0 & 0 \\ -\nu_{XY}/E_X & 1/E_Y & -\nu_{ZY}/E_Z & 0 & 0 & 0 \\ -\nu_{XZ}/E_X & -\nu_{YZ}/E_Y & 1/E_Z & 0 & 0 & 0 \\ 0 & 0 & 0 & 1/G_{XY} & 0 & 0 \\ 0 & 0 & 0 & 0 & 1/G_{YZ} & 0 \\ 0 & 0 & 0 & 0 & 0 & 1/G_{ZX} \end{bmatrix} \begin{bmatrix} \sigma_X \\ \sigma_Y \\ \sigma_Z \\ \tau_{XY} \\ \tau_{YZ} \\ \tau_{ZX} \end{bmatrix} \tag{8}$$

Because $S_{ij} = S_{ji}$ relation between Poisson's ratios ν_{ij} and ν_{ji} is expressed by

$$\frac{\nu_{XY}}{E_X} = \frac{\nu_{YX}}{E_Y}, \qquad \frac{\nu_{YZ}}{E_Y} = \frac{\nu_{ZY}}{E_Z}, \qquad \frac{\nu_{ZX}}{E_Z} = \frac{\nu_{XZ}}{E_X}. \tag{9}$$

In this study the Young's moduli (Table 5) were determined from tension and compression tests on cubic samples. Shear moduli G_{ZX} and G_{YZ} (Table 6) were evaluated from bending tests. All samples were cut out from the panel (Fig. 3). The limited thickness of the panel did not allow to use similar methods for identification of the shear modulus G_{XY} in X-Y plane. The authors carried out tension and compression tests in direction oriented at 45^0 to the principal material coordinates X and Y (Fig. 6). The Young's modulus $(E_X)_{45^\circ}$ determined on cubic samples allows to evaluate G_{XY} from the formula (10) given by Daniel (Daniel and Ishai 1994)

$$\frac{1}{G_{XY}} = \frac{4}{(E_X)_{45^\circ}} - \frac{1-\nu_{XY}}{E_X} - \frac{1-\nu_{YX}}{E_Y}. \tag{10}$$

Table 7 Experimental results of Young's modulus $(E_X)_{45°}$ in *X*-*Y* plane

	TENSION	COMPRESSION
$(E_X)_{45°}$ [MPa]	9.09	6.51
	8.97	6.08
	9.78	6.00
	9.90	6.56
	10.39	6.76
	9.68	6.91
Mean value	**9.63**	**6.47**
Standard deviation	0.49	0.33

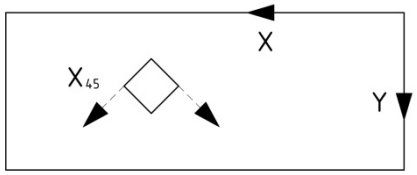

Fig. 6 *X*-*Y* plane and sample

The tension and compression tests carried out in three directions *X*, *Y* and *Z* revealed that the Young's modulus *E* of PU foam depends not only on the direction but also on the sign of stress. The most evident difference between E_{Ct} and E_{Cc} (Table 5) was observed in *Y* direction. The orthotropic model with coefficients dependent on the sign of stress would be rather unpractical, therefore at the present study the compliance coefficients in Eq. (8) are proposed as arithmetic mean values obtained in tension and compression tests. Moreover, zero Poisson's ratios $\nu_{XY} = \nu_{YZ} = \nu_{ZX}$ are assumed. Zero Poisson's ratios were observed in compression tests carried out in this study and also mentioned by Mills (2007). Basing on these assumptions we arrive at the following compliance matrix S_{ij} in Eq. (8)

$$\begin{bmatrix} \varepsilon_X \\ \varepsilon_Y \\ \varepsilon_Z \\ \gamma_{XY} \\ \gamma_{YZ} \\ \gamma_{ZX} \end{bmatrix} = \begin{bmatrix} 1/[13.89] & 0 & 0 & 0 & 0 & 0 \\ 0 & 1/[5.61] & 0 & 0 & 0 & 0 \\ 0 & 0 & 1/[3.54] & 0 & 0 & 0 \\ 0 & 0 & 0 & 1/[4.05] & 0 & 0 \\ 0 & 0 & 0 & 0 & 1/[2.30] & 0 \\ 0 & 0 & 0 & 0 & 0 & 1/[3.00] \end{bmatrix} \begin{bmatrix} \sigma_X \\ \sigma_Y \\ \sigma_Z \\ \tau_{XY} \\ \tau_{YZ} \\ \tau_{ZX} \end{bmatrix} \tag{11}$$

The coefficient $S_{44} = 1/G_{XY}$ was evaluated from Eq. (10) where $(E_X)_{45°} = 8.05$ MPa was introduced (arithmetic mean values obtained in tension and compression tests – Table 7)

$$\frac{1}{G_{XY}} = \frac{4}{8.05} - \frac{1-0}{13.89} - \frac{1-0}{5.61} = 0.24665 \quad \Rightarrow \quad G_{XY} = 4.05 \text{ MPa} \tag{12}$$

5. Numerical analysis

In the present chapter the models of PU foam will be verified by the example of a four-point bending test. The sample is denoted as No. (5) in Fig. 3 and the scheme of the test is shown in Fig. 7. The beam had following dimensions: thickness of the core d_C = 94.36 mm, width B = 100 mm, the total length L = 1000 mm, the length of span L_0 = 900 mm and the thickness of steel facings t = 0.35 mm.

Three laboratory tests have been done. The averaged deflection w of the midpoint of the span as a function of the load F is presented in Fig. 8 and is labelled No. 0. Next plots represent numerical solutions obtained using ABAQUS FEM program. Facings were modelled as four node, doubly curved, thin or thick shell, finite membrane strains elements S4. The core was modelled using eight node linear brick elements C3D8. Support conditions refer to experimental scheme in Fig. 7. The panel is supported by two basing plates modelled as rigid bodies. For both supporting base plates all three translations and rotations with respect to axes X and Z are equal to zero and free rotations with respect to the axis Y were assumed. The connection between the plate and the support was defined as a contact 'surface to surface' with friction coefficient equal to 0.3.

In numerical analyses it was assumed that the facings are flat and made of steel with Young's modulus E_F = 210 GPa and Poisson's ratio ν_F = 0.3. All numerical analyses were done in linear-elastic range. The following examples were solved for different material parameters of the PU core.

- **Example 1**. Linear, elastic, orthotropic. Material parameters as in Eq. (11), where the shear moduli G_{YZ} = 2.30 MPa, and G_{ZX} = 3.0 MPa were obtained from bending tests.
- **Example 2**. Linear, elastic, orthotropic. Material parameters as in Eq. (11), but the shear moduli G_{YZ} = 2.20 MPa, and G_{ZX} = 2.49 MPa were taken from double-lap shear tests.
- **Example 3**. Linear, elastic, isotropic. Material parameters: G_C = 3.0 MPa from Table 6, hence fictitious value E_C = 6.0 MPa obtained from in Eq. (6) had to be introduced with ν_C = 0.
- **Example 4**. Linear, elastic, isotropic. Material parameters: G_C = 2.49 MPa from Table 6, hence fictitious value E_C = 4.98 MPa obtained from Eq. (6) had to be introduced with ν_C = 0.
- **Example 5.** Material parameters: E_C = 3.54 MPa from in Eq. (11) with ν_C = 0, hence it would be G_C = 1.77 MPa.

Obtained results are shown in Fig. 8. All plots, experimental and numerical ones, represent the deflection w after subtraction the support compression w_0 from total displacement f of the midpoint of the span.

Plot 1 representing the orthotropic model with compliance matrix Eq. (11) and plot 3 representing isotropic model with G_{ZX} = 3.0 MPa agree very well with the experimental plot 0 in

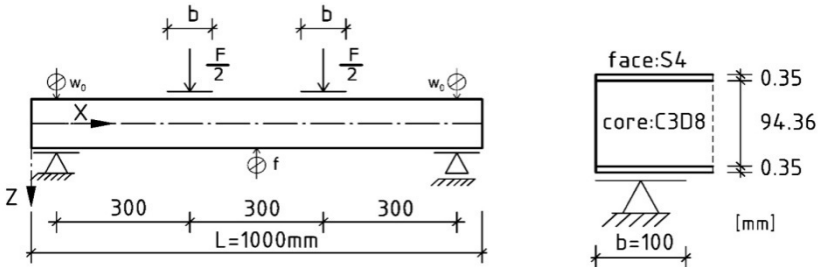

Fig. 7 (a) The scheme of the tested sample; (b) Close-up of the support area

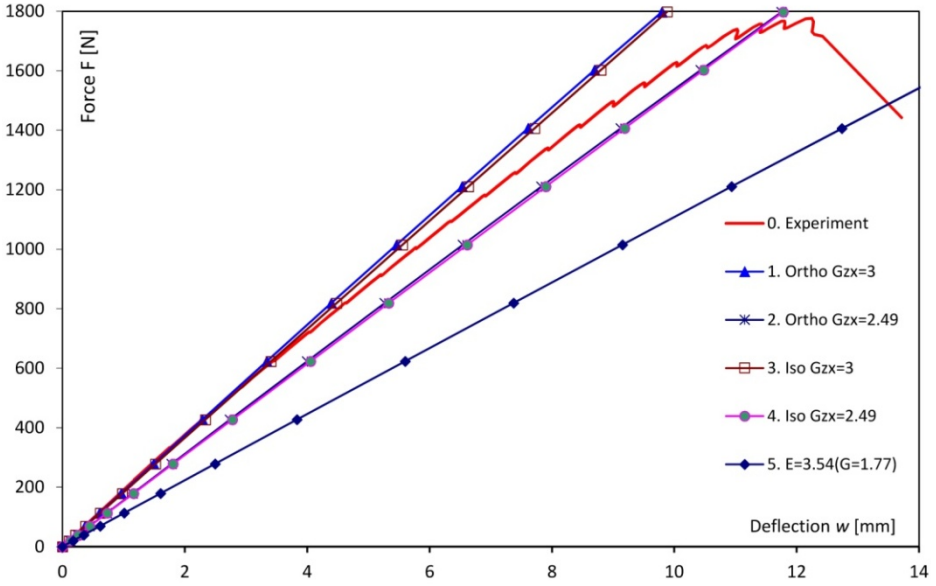

Fig. 8 Four-point bending test. FEM solutions No 1-5 versus experimental plot No 0

its initial linear range. Comparison of plots 1 and 3 with the experimental plot 0 demonstrates satisfactory agreement for low range of load. For higher load levels the plot 0 reveals the non-linearity of the structural response. It must be assigned to the PU foam in the core because at the load F = 1000 N the stress in steel facings is 45 MPa that is much below elasticity limit. The non-linear behaviour was not manifested in case of long panels because of lower stresses in the core. Since all numerical analyses are based on linear physical laws, let us confine next discussion to the initial state of loading. When we implemented the shear moduli obtained from double-lap tests then plot 2 representing the orthotropic model Eq. (11) with shear moduli G_{YZ} = 2.20 MPa and G_{ZX} = 2.49 MPa and plot 4 for isotropic model with G_{ZX} = 2.49 MPa described softer structural responses than the experimental plot 0. Note that in order to create a linear elastic isotropic FEM model with the required shear modulus G one has to define input data with fictitious Young's modulus E. Plot 5 illustrates how erroneous the FEM model would be when the user of computer program defines the PU core by direct introduction it's Young's modulus E obtained from the tension/compression test recommended in the code.

6. Conclusions

The foaming processes in PU foam used in the production of sandwich panels often result in the formation of elongated cells in the foam. In effect the stress-strain relations depend on the stress direction, what has been shown in this paper. The linear elastic response of the foam is observed only at low range of strains less than 10%. This range also depends on the direction of stress.

Anisotropic material models need a set of parameters and require numerous experimental tests. Therefore, many papers and codes regard cellular foams as an elastic and isotropic material. The present work demonstrates that this assumption has to be used with limited confidence. The paper

also demonstrated that PU foam is not homogeneous in the direction of slab's width although the tested slabs were made by a producer of high technology level. This fact should be taken into account in the analysis of local effects e.g. bubbles. In other analyses the material parameters averaged over the width of slab should be used.

Acknowledgments

The research described in this paper was financially supported by Poznan University of Technology 01/11/DSPB/0304.

References

Allen, H.G. (1969), *Analysis and Design of Structural Sandwich Panels*, Pergamon Press, London, UK.

Awad, Z.K. (2013), "Optimization of a sandwich beam design: Analytical and numerical solutions", *Struct. Eng. Mech., Int. J.*, **48**(1), 93-102.

Caliri Júnior, M.F., Soares, G.P., Angélico, R.A., Bresciani Canto, R. and Tita, V. (2012), "Study of an anisotropic polymeric cellular material under compression loading", *J. Mater. Res.*, **15**(3), 359-364.

Chen, L. and Fatt, M.S.H. (2013), "Transversely isotropic mechanical properties of PVC foam under cyclic loading", *J. Mater. Sci.*, **48**(19), 6786-6796.

Chuda-Kowalska, M. (2012), "Influence of longitudinal edge profiling in sandwich panels on interpretation of experimental results", *Scientific Research of the Institute of Mathematics and Computer Science*, **4**(11), 19-27.

Chuda-Kowalska, M. (2013), "Methodology of Experimental Tests of Three-layered Panels with Thin Facings", Poznan University of Technology, Poznan, Poland. [In Polish]

Chuda-Kowalska, M., Pozorski, Z. and Garstecki, A. (2010), "Experimental determination of shear rigidity of sandwich panels with soft core", *Proceedings of the 10th International Conference Modern Buildings Materials*, *Structures and Techniques*, Vilnius, Lithuania, May.

Chuda-Kowalska, M., Gajewski, T. and Garbowski, T. (2015), "Mechanical characterization of orthotropic elastic parameters of a foam by the mixed experimental-numerical analysis", *J. Theor. Appl. Mech.*, **53**(2), 383-394.

Daniel, I. and Ishai, O. (1994), *Engineering Mechanics of Composite Materials*, Oxford University Press.

Davies, J.M. (Editor) (2001), *Lightweight Sandwich Constructions*, Blackwell Science Ltd.

EN 14509 (2013), Self-supporting double skin metal faced insulating panels – Factory made products – Specifications.

Gibson, R. (2011), "A simplified analysis of deflections in shear deformable composite sandwich beams", *J. Sandw. Struct. Mater.*, **13**(5), 579-588.

Gibson, L. and Ashby, M. (1997), *Cellular Solids. Structure and Properties*, Cambridge University Press.

Gosowski, B. and Gosowski, M. (2014), "Exact solution of bending problem for continuous sandwich panels with profiled facings", *J. Construct. Steel Res.*, **101**, 53-60.

Hassinen, P., Martikainen, L. and Berner, K. (1997), "On the design and analysis of continuous sandwich panels", *Thin-Wall. Struct.*, **29**(1-4), 129-139.

Janus-Michalska, M. and Pecherski, R.B. (2003), "Macroscopic properties of open-cell foams based on micromechanical modelling", *Technische Mechanik*, **23**(2/4), 221-231.

Jin, H., Lu, W.-Y., Scheffel, S. and Hinnerichs, T.D. (2007), "Full-field characterization of mechanical behavior of polyurethane foams", *Int. J. Solid. Struct.*, **44**(21), 6930-6944.

Juntikka, R. and Hallstorm, S. (2007), "Shear characterization of sandwich core materials using four-point bending", *J. Sandw. Struct. Mater.*, **9**(1), 67-94.

Liu, Q. and Subhash, G. (2004), "A phenomenological constitutive model for foams under large

deformations", *Polym. Eng. Sci.*, **44**(3), 463-473.
Mills, N.J. (2007), "*Polymer Foams Handbook. Engineering and Biomechanics Applications and Design Guide*", Butterworth – Heinemann.
Plantema, F.J. (1966), *Sandwich Construction*, John Wiley & sons, New York, NY, USA.
Pokharel, N. and Mahendran, M. (2005), "An investigation of lightly profiled sandwich panels subjected to local buckling and flexural wrinkling effects", *J. Construct. Steel Res.*, **61**(7), 984-1006.
Rzeszut, K., Garstecki, A. and Czajkowski, A. (2014), "Parameter identification in FEM models of thin-walled purlins restrained by sheeting", *Rec. Adv. Computat. Mech.*, *CRC Press/Balkema*, pp.121-128.
Studziński, R., Pozorski, Z. and Garstecki, A. (2013), "Sensitivity analysis of sandwich beams and plates accounting for variable support conditions", *Bulletin of the Polish Academy of Sciences - Technical Sciences*, **61**(1), 201-210.
Studziński, R., Pozorski, Z. and Garstecki, A. (2015), "Structural behavior of sandwich panels with asymmetrical boundary conditions", *J. Construct. Steel Res.*, **104**, 227-234.
Subramanian, N. and Sankar, B.V. (2012), "Evaluation of micromechanical methods to determine stiffness and strength properties of foams", *J. Sandw. Struct. Mater.*, **14**(4), 431-447.
Tita, V. and Caliri Júnior, M.F. (2012), "Numerical simulation of anisotropic polymeric foams", *Latin American Journal of Solids and Structures*, **9**(2), 259-279.
Xie, Z., Yan, Q. and Li, X. (2014), "Investigation on low velocity impact on a foam core composite sandwich panel", *Steel Compos. Struct., Int. J.*, **17**(2), 159-172.
Zenkert, D. (1995), *An Introduction to Sandwich Construction*, EAMS.
Ziolkowski, A. (2006), "Simple shear test in identification of constitutive behaviour of materials submitted to large deformations – hyperelastic materials case", *Eng. Transact.*, **54**(4), 251-269.

CC